

Compact printed hexagonal ultra wideband monopole antenna with band-notch characteristics

Ankan Bhattacharya^{a*}, Bappaditya Roy^a, Santosh K Chowdhury^b & Anup K Bhattacharjee^a

^aDepartment of Electronics and Communication Engineering, National Institute of Technology, M G Road, Durgapur 713 209, India

^bDepartment of Electronics and Telecommunication Engineering, Jadavpur University, R S C Mallick Road, Kolkata 700 032, India

Received 7 June 2017; accepted 12 October 2018

This article presents a compact, printed hexagonal monopole, ultra wideband antenna along with band-notch characteristics. The proposed monopole antenna consists of a printed hexagonal radiating element and a defected ground structure. Printed round-slot geometry and defected ground structure play a vital role in achieving the ultra wide bandwidth. Band-notch characteristics for eliminating the interference arising from the existing WLAN (5.15 – 5.825 GHz) band has been incorporated in the antenna frequency response by the insertion of C-shaped stubs near the feeding segment. The antenna shows a decent gain of ≥ 3.0 dBi throughout the entire bandwidth except at the notched frequency band. Measured results agree well with the simulated values.

Keywords: Ultra-wideband, Monopole antenna, Round-slot geometry, Defected ground structure, Band-notch characteristics

1 Introduction

In modern communication system, various types of slot geometries play an important role in microstrip patch antennas to obtain a larger bandwidth and several other useful features. The technology¹ has rapidly developed since FCC released the band from 3.1-10.6 GHz for ultra wideband (UWB) systems in 2002. There is a huge demand for ultra wideband antennas in the field of wireless communication because of high data rate, cost effective and very low power consumption feature². Earlier, researches used to follow the CPW technique for generating the wide band frequency range. Fallahi *et al.*³ presented a CPW fed monopole antenna which covered the 3.1-10.6 GHz frequency range. An UWB monopole antenna has been presented by Jilkova *et al.*⁴, in which some experimental comparisons are shown. Natarajamani *et al.*⁵ presented a compact, planer antenna for triple-band characteristics with a good arrangement for wireless communication. Here an octagonal shaped patch structure has been used by etching two C-shaped slots for the proposed antenna. A low-profile double cross patch for dual-band monopole antenna has been proposed by Khalily *et al.*⁶ The structure excited a TM_{01} mode, but the antenna suffers from

low bandwidth. Several wide band monopole antennas embedded with different slots like rectangular, square, circular, triangular shapes have been presented in earlier studies^{7,8}. Several types of wideband antennas with slot geometries are also available in literature⁹⁻¹⁵ for achieving the wide bandwidth. However, all of these proposed designs are not compact and in the most cases the technique of eliminating the interference from the WLAN (5.15 – 5.825 GHz) band has been neglected. In this article a compact, printed, hexagonal monopole, ultra wideband antenna along with band-notch feature has been presented. The proposed monopole antenna consists of a printed hexagonal radiating element and a defected ground structure. Printed round-slot geometry and defected ground structure play a vital role in achieving the ultra wide bandwidth. Band-notch characteristics for eliminating the interference arising from the existing WLAN (5.15-5.825 GHz) band has been incorporated in the antenna frequency response by the insertion of C-shaped stubs near the feeding segment. The antenna shows a decent gain of ≥ 3.0 dBi throughout the entire bandwidth except at the notched frequency band.

2 Proposed Design

Initially a printed hexagonal monopole antenna (Antenna 1) has been designed which is displayed in

*Corresponding author (E-mail: bhattacharya.ankan1987@gmail.com)

Fig. 1. The design consists of a hexagonal radiating element incorporated with circular slots, which forms a ring like pattern. The design consists of a partial ground plane with a rectangular slot placed at the centre. This type of ground structure is known as defected ground structure in antenna engineering. Teflon (PTFE) which has a dielectric constant of 2.1 and a loss tangent of 0.02 has been used as the dielectric material. The overall dimension of the structure has been kept as $W \times L = 21.25 \times 32.75 \text{ mm}^2$. The feed line has been designed to approximately match the 50Ω characteristic impedance using Eqs (1) and (2).

For the proposed design, substrate dielectric constant, $\epsilon_r = 2.1$, substrate height, $h = 1.0 \text{ mm}$ and width of the feed line, $Fw = 2.8 \text{ mm}$.

$$\epsilon_{eff} = \frac{\epsilon_r + 1}{2} + \frac{\epsilon_r - 1}{2} [\sqrt{1 + 12(h/Fw)}]^{-1} \quad \dots (1)$$

$$Z_o = \frac{120\pi}{\sqrt{\epsilon_{eff}} [\frac{Fw}{h} + 1.39 + 0.66 \ln(\frac{Fw}{h} + 1.44)]} \quad \dots (2)$$

for $Fw/h \geq 1$.

Z_o is the characteristic-impedance and ϵ_{eff} is the effective dielectric constant of substrate¹⁵.

The hexagonal radiating element is made up of copper (annealed) in which circular slots have been embedded. The slots at each corner of the radiating element are 3.0 mm in diameter each, whereas the one at the centre is 4.25 mm in diameter. The ground plane (copper) of the proposed structure is in the form of a rectangular strip with dimensions of $21.25 \times 9.75 \text{ mm}^2$. The thickness of the structure has been kept equal to 2.0 mm. A rectangular slot of dimension $2.8 \times 7.00 \text{ mm}^2$ has been etched from the centre of the ground plane for improvement in frequency response.

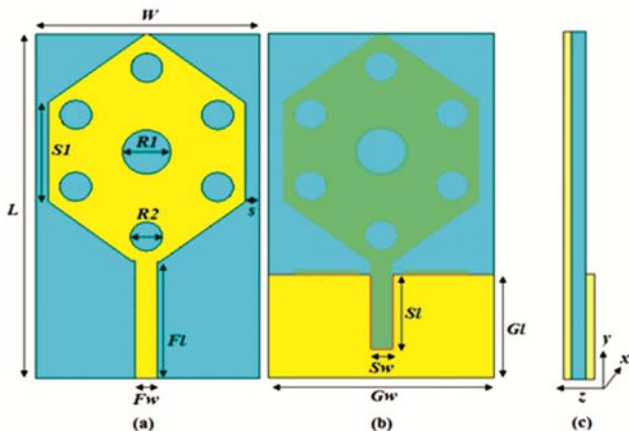


Fig. 1 – UWB printed hexagonal monopole antenna (Antenna 1) (a) front view, (b) rear view and (c) side view.

The various dimensions of the proposed structure are $W = 21.25 \text{ mm}$, $L = 32.75 \text{ mm}$, $Fw = 2.8 \text{ mm}$, $Fl = 10.25 \text{ mm}$, $SI = 9.75 \text{ mm}$, $R1 = 4.0 \text{ mm}$, $R2 = 3.0 \text{ mm}$, $s = 1.0 \text{ mm}$, $Sw = 2.8 \text{ mm}$, $SI = 7.00 \text{ mm}$, $Gw = 21.25 \text{ mm}$ and $Gl = 9.75 \text{ mm}$.

A prototype of Antenna 1 has been fabricated. The results have been measured using vector network analyzer (VNA). The simulated and measured results show a good agreement between them. Slight deviation may be due to the effect of soldering and fabrication tolerance. Figure 2 shows the front and rear views of the fabricated prototype antenna with printed hexagonal radiating element and slotted ground plane.

3 Results and Discussion

3.1 Return loss characteristics

Figure 3 shows the comparison plot of measured and simulated return losses. The return loss, i.e., $|S_{11}|$

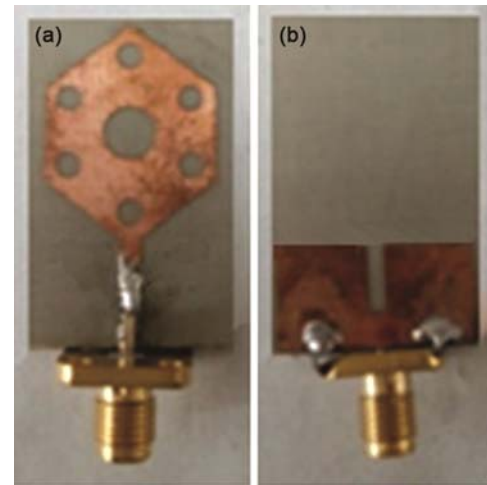


Fig. 2 — Antenna 1 fabricated prototype (a) front view and (b) rear view.

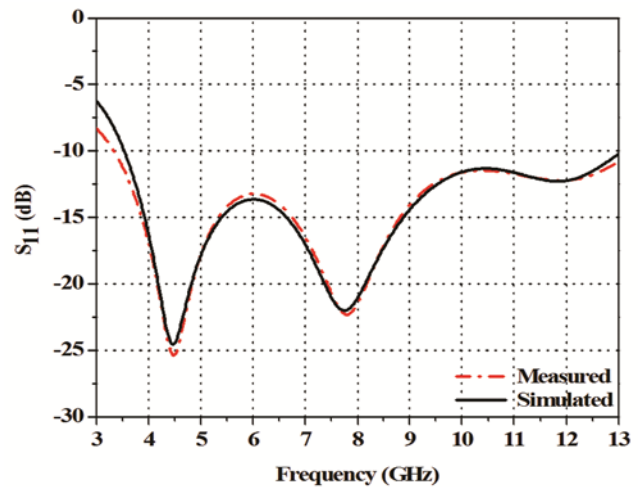


Fig. 3 — Measured and simulated return losses of Antenna 1.

characteristics shows that an impedance bandwidth of 9.9 GHz (3.1 - 13.0 GHz) has been obtained. Results of simulation and measurement show a good agreement between them. The maximum value of the return loss $|S_{11}|$ obtained is > 25 dB at a frequency of about 4.5 GHz. The proposed structure therefore satisfies the bandwidth required for ultra wideband communication (3.1 – 10.6 GHz) as prescribed by the FCC (Federal Communications Commission)¹. Presence of circular slots on the hexagonal radiating element is responsible for the generation of ultra wide bandwidth, which has been discussed in the following section.

3.2 Effect of circular-slots in the radiating element

The effect of introducing circular slots in the radiating element has been studied in this section. Figure 4 shows the S_{11} versus frequency plot with and without the presence of circular slots in the radiating element. Comparatively wider bandwidth has been observed due to the existence of circular slots in the metallic radiator. The diameters of the circular slots namely $R1$ and $R2$ have been optimized to obtain the best result. After several parametric variations the dimensions of the circular slots have been considered as $R1 = 4.0$ mm and $R2 = 3.0$ mm for optimum response. On observation of the antenna surface current distribution pattern, it can be observed that the surface current is concentrated around the edges of the circular slots. The presence of circular slots disturbs the even distribution of surface current on the surface of the radiator. The generated resonant modes, thereby come closer to one another, resulting in an ultra wide bandwidth of 9.9 GHz (3.1 - 13.0 GHz).

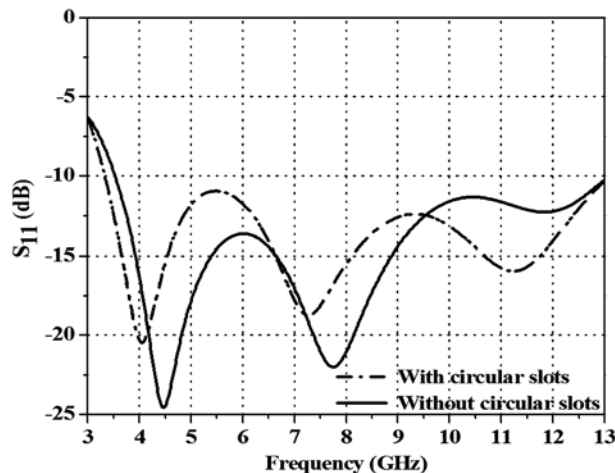


Fig. 4 – Frequency response of Antenna 1 with/without circular slots.

3.3 Effect of slot dimension on antenna response

The diameters of the circular slots $R1$ and $R2$ on the hexagonal radiating element play a significant role governing the frequency response characteristics of the antenna under consideration. Figure 5 shows the variation of slot diameter on the antenna frequency response. Desired response has been achieved when $R1$ and $R2$ have been chosen as 4.0 mm and 3.0 mm, respectively.

3.4 Effect of open-circuited stubs

Now, our objective is to introduce a band-notch feature in the WLAN (5.15 – 5.825 GHz) region for eliminating the interference effect. Open circuited stubs are useful in creating band-notch frequency. For this purpose we have introduced two C-shaped open-circuited stubs beside the feeding segment of Antenna 1.

Figure 6 shows the modified structure (Antenna 2) after the introduction of two C-shaped open circuited

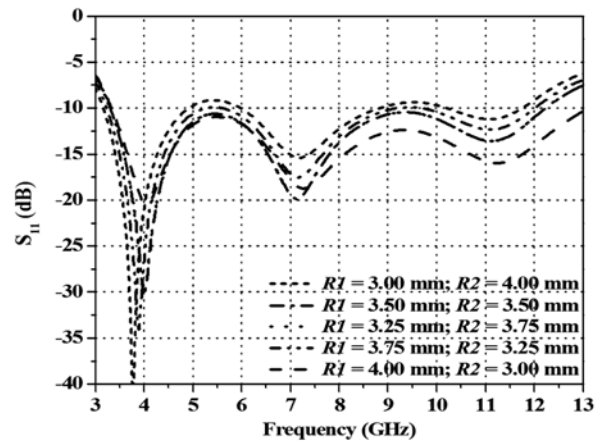


Fig. 5 – Frequency response of Antenna 1 for different values of $R1$ and $R2$.

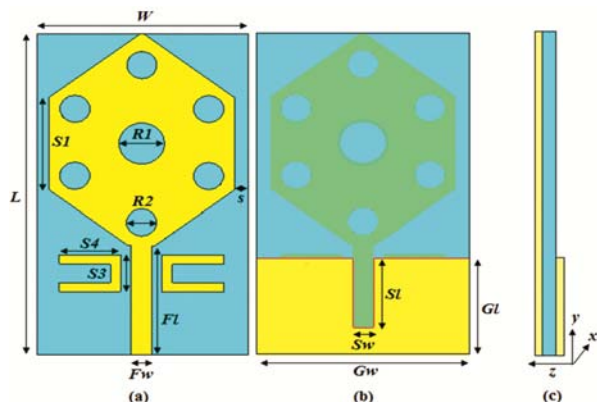


Fig. 6 – Proposed monopole antenna with two C-shaped stubs (Antenna 2) (a) front view, (b) rear view and (c) side view.

stubs beside the feeding segment and Fig. 7 shows the fabricated prototype. The design is simulated and the simulated result has been compared with the measured values.

Figure 8 shows the frequency response characteristics of Antenna 2. A band-notch feature has been obtained in the 4.5 – 5.85 GHz range for elimination of the interference from the existing WLAN band (5.15 – 5.825 GHz) due to the incorporation of two open-circuited C-shaped stubs at the two sides of the feeding segment. The perimeter of the stub is approximately equal to the quarter guide wavelength at the desired notch frequency. The guide wavelength is expressed as:

$$\lambda_g = \frac{c}{f_{notch} \sqrt{\epsilon_{eff}}} \quad \dots (3)$$

where c is the velocity of light in vacuum, f_{notch} is the centre frequency of the notch band and ϵ_{eff} is the

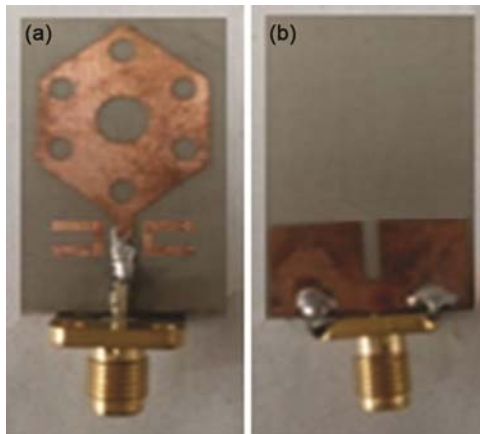


Fig. 7 – Antenna 2 fabricated prototype with C-shaped stubs (a) front view and (b) rear view.

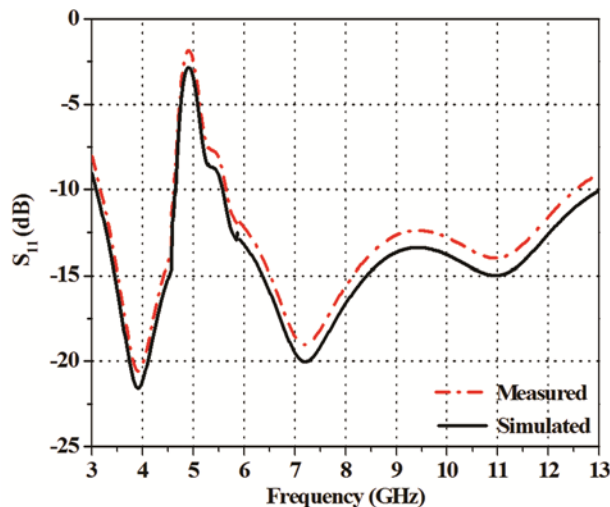


Fig. 8 – Antenna 2 with band-notch characteristics.

effective relative permittivity of the substrate. The band-notch frequency can be fine-tuned by adjustment of the dimensions $S3$ and $S4$ of the open-circuited stubs. $S3$ (= 3.75 mm) and $S4$ (= 7.5 mm) has been optimized to obtain the band-notch frequency centered at 5.2 GHz.

3.5 Group delay plot of proposed antenna

The degree of signal distortion can be known from the group delay factor. It gives a measure of the slope of the transmission phase response of the signal.

A constant value is obtained from conversion of the linear section of the phase response of the signal under consideration and the deviations in phase are transformed to deviations from the constant group delay factor. Group delay can be expressed as:

$$\text{Group delay} = - \frac{\Delta\phi}{\Delta\omega} \quad \dots (4)$$

where $\Delta\phi$ and $\Delta\omega$ are the phase and frequency deviations of the signal, respectively. The group delay changes abruptly at the band-notch frequency point. Figure 9 shows the group delay plot of Antenna 2, which shows an acceptable performance in time-domain, except at the band-notch frequency point (s).

3.6 Gain characteristics of proposed antenna

The proposed antenna shows a decent gain of ≥ 3.0 dBi throughout the entire operation bandwidth. However the antenna gain falls below the 0 dBi value at the band-notch frequency point (Fig. 10).

The effect can be well understood from observation of the antenna surface current distribution pattern (Fig. 11). It can be observed from Fig. 11 (c), that the

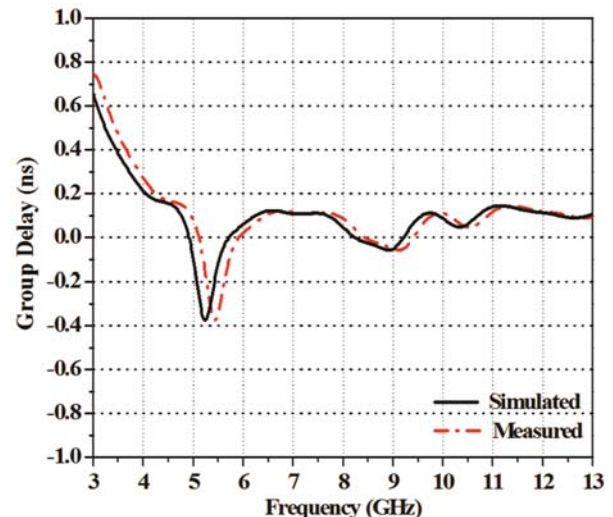


Fig. 9 – Group delay plot of Antenna 2 (simulated and measured).

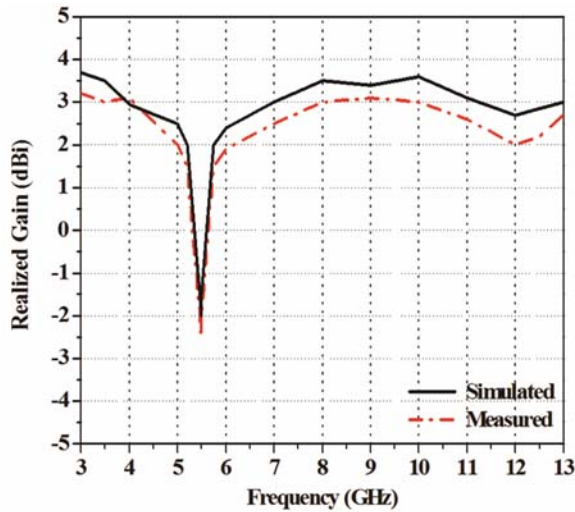


Fig. 10 – Gain characteristics of Antenna 2 (simulated and measured).

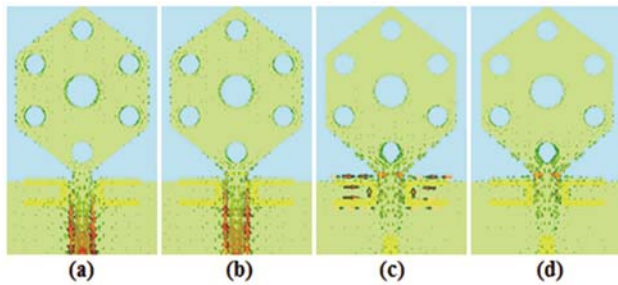


Fig.11 – Antenna 2, surface current distribution pattern at (a) 2.1 GHz, (b) 3.4 GHz, (c) 5.2 GHz and (d) 11.0 GHz.

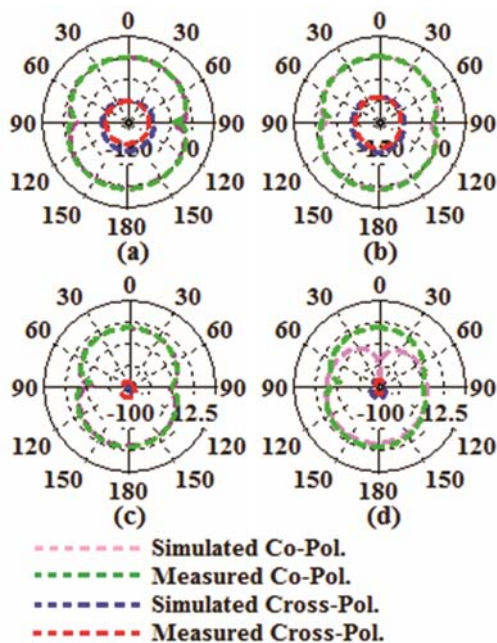


Fig. 12 – Measured 2-D radiation pattern of Antenna 2 at (a) 2.1 GHz, (b) 3.4 GHz, (c) 5.2 GHz and (d) 11.0 GHz.

surface current is concentrated near the edges of the C-shaped open-circuited stubs located beside the feeding segment. The presence of stubs disturbs the surface current distribution and is responsible for generation of band-notch frequency in the 4.5 – 5.85 GHz range, for eliminating the interference from the WLAN band.

The antenna radiation pattern has been displayed in Fig. 12. Effective Co-Pol. and Cross-Pol. patterns has been obtained for $\theta = 0^\circ$ and $\theta = 90^\circ$. It may be observed that the radiation patterns are somewhat omni-directional in nature.

4 Conclusions

In this article a compact, printed hexagonal monopole, ultra wideband antenna with band-notch feature has been investigated. The antenna has a band-notch frequency in the 4.5 – 5.85 GHz range, centered at 5.2 GHz for elimination of the interference arising from the existing WLAN band (5.15 – 5.825 GHz). The proposed monopole satisfies all the necessary specifications of a typical monopole antenna in perspective of return loss, gain and effective time-domain response. Band notch characteristic is an added advantage. Therefore the proposed antenna is no doubt an attractive candidate for wireless communications supporting an ultra wide bandwidth.

Acknowledgment

The authors would like to express sincere gratitude to Dr. Pranab Paul of Microline India, Kolkata for extending help in device fabrication and provision of measurement facilities.

References

- 1 FCC 02-48, Washington D C 20554 (Datasheet), Released On April 22, 2002. https://Transition.FCC.Gov/Bureaus/Engineering_Technology/Orders/2002/FCC02048.pdf.
- 2 Hazdra P, Capek M, Masek M & Lonsky T, *Radioengineering*, 25 (2016) 12.
- 3 Fallahi H & Atlasbaf Z, *IEEE Antennas Wireless Propag Lett*, 12 (2013) 1484.
- 4 Jilkova J & Raida Z, *Radioengineering*, 17 (2007) 37.
- 5 Natarajamani S, Behera S K & Patra S K, *Microwave Opt Technol Lett*, 54 (2012) 539.
- 6 Tak J, Kang D & Choi J, *Microwave Opt Technol Lett*, 56 (2014) 2929.
- 7 Khalil M, Rahim M K A, Kishk A A & Danesh S, *Radioengineering*, 22 (2013) 281.
- 8 Akbari M, Koohestani M, Ghobadi C & Nournia J, *Int J RF Microwave Comput-Aided Eng*, 21 (2011) 216.
- 9 Amman M J, *Microwave Opt Technol Lett*, 30 (2001) 229.
- 10 Chiou J Y & Wong K L, *IEEE Trans Antennas Propag*, 51 (2003) 719.

- 11 Chen H D, *IEEE Trans Antennas Propag*, 51 (2003) 1982.
- 12 Jan J Y & Hsiang C Y, *IET Electron Lett*, 42 (2006) 1377.
- 13 Roy B, Bhattacharya A, Bhattacharjee A K & Chowdhury S K, *Indian J Sci Technol*, 8 (2015) 30.
- 14 Chatterjee S, Chowdhury S K, Sarkar P P & Sarkar D C, *Indian J Pure Appl Phys*, 51 (2013) 800.
- 15 Naghshvarian J M, *IEEE Trans Antennas Propag*, 56 (2008) 3844.